SRSF3 promotes the generation of XBP1s to stabilize autophagy and enhance hypoxia adaptation in glioma

Bohu Liu,[1,2,3]* Xiaoran Zhang,[4]* Jintao Tian,[1,2] Xiaobin Huang,[1] Xuhui Li,[1] Jinxi Zhao,[1] Zhenghu Xu,[1] Jun Pu[1,2]

[1]Neurosurgery Department, The Second Affiliated Hospital of Kunming Medical University, Kunming, Yunnan
[2]Kunming Medical University National Health Commission Laboratory for Drug Dependence and Withdrawal, Kunming, Yunnan
[3]Neurosurgery Department, Ganmei Hospital Affiliated to Kunming Medical University, Kunming, Yunnan
[4]Critical Care Medicine Department, The Second Affiliated Hospital of Kunming Medical University, Kunming, Yunnan, China

These authors contributed equally to this study

ABSTRACT

Hypoxia is a key driver of glioblastoma (GBM) progression. Serine/arginine-rich splicing factor 3 (SRSF3) is associated with the malignant progression of GBM, but its role in the hypoxic microenvironment of GBM remains unclear. This study aimed to explore the regulatory role and molecular mechanisms of SRSF3 in hypoxia adaptation in GBM. The expression of SRSF3 in normal astrocytes and GBM cells was detected. The effects of knockdown or overexpression of SRSF3 combined with hypoxia treatment on malignant phenotypes and hypoxia stress adaptation in GBM cells were evaluated. Cell viability, colony formation, migration, invasion, and cell death assays were performed to assess phenotypic changes. Mechanisms were investigated using mRFP-GFP-LC3, autophagy, and unfolded protein response (UPR)-related molecular detection. SRSF3 was highly expressed in GBM cells. Knockdown of SRSF3 inhibited cell viability, migration, invasion, and colony formation, whereas overexpression of SRSF3 promoted malignant behaviors. Further studies revealed that hypoxia induction significantly increased the expression levels of GRP78, CHOP, ATF4, LC3-II/I, and p62; upregulated the GFP/mRFP ratio; and increased cleaved-caspase3 expression, promoting cell death. Mechanistic studies revealed that SRSF3 overexpression promoted XBP1s formation, alleviated hypoxia-induced autophagic flux blockage, and reduced cell death. The IRE1 RNase inhibitor 4μ8C weakened the SRSF3-mediated promotion of XBP1s generation. SRSF3 enhances adaptive UPR output by promoting IRE1-dependent XBP1 splicing, thereby maintaining autophagic flux and promoting GBM cell survival under hypoxic conditions.

Key words: Glioma; glioblastoma; SRSF3; hypoxia; autophagy; XBP1s.

Correspondence: Jun Pu, Neurosurgery Department, The Second Affiliated Hospital of Kunming Medical University, Kunming, Yunnan 650000, China. E-mail: Pujun137@126.com
Zhenghu Xu, Neurosurgery Department, The Second Affiliated Hospital of Kunming Medical University, Kunming, Yunnan 650000, China. E-mail: 15567662276@163.com

Contributions: Bohu Liu, Jun Pu, conceptualization. Xiaoran Zhang, Jintao Tian, Zhenghu Xu, formal analysis. Bohu Liu, Xiaobin Huang, data acquisition, methodology, writing-original draft. Jun Pu, funding acquisition, resources, project administration. Xuhui Li, software. Xiaoran Zhang, Jintao Tian, validation. Jinxi Zhao, visualization. Zhenghu Xu, Jun Pu, writing-review and editing. All the authors contributed substantially to this manuscript, read and approved the final manuscript.

Conflict of interest: the authors declare that no competing interests, and all authors confirm accuracy.

Availability of data and materials: the data are available from the corresponding author upon reasonable request.

Funding: this study was supported by the National Natural Science Foundation of China (82160512); the First-Class Discipline Team of Kunming Medical University (2024XKTDYS06); Yunnan Fundamental Research Projects (202401AS070018); Yunnan Fundamental Research Kunming Medical University Joint Projects (202401AY070001-002X); the NHC Key Laboratory of Drug Addiction Medicine (K1323303, KN202417); Kunming City Medical Science and Technology Talents in Reserve (2025-sw(reserve)-05); and the Research Fund Project of the Education Department of Yunnan Province (2026J 0306).

Introduction

Glioma is the most common primary malignant tumor of the central nervous system and accounts for 80–85% of all brain tumors.[1] Glioblastoma (GBM), the highest grade (WHO grade 4) astrocytoma, poses significant public health challenges because of its high degree of malignancy, rapid progression, short survival period, and poor prognosis.[2] Studies have shown that approximately two-thirds of patients survive no more than two years after diagnosis, and high treatment costs impose a substantial burden on patients.[3,4] Therefore, there is an urgent need to clarify its key pathogenic mechanisms and develop targeted therapeutic strategies. Hypoxia is a core microenvironmental feature of GBM and promotes tumor invasion, treatment resistance, and recurrence.[5,6] However, the underlying mechanisms by which hypoxia drives the malignant behavior of GBM remain incompletely understood.

GBM exists in a long-lasting hypoxic microenvironment, and hypoxia inevitably induces endoplasmic reticulum stress (ERS) and activates the unfolded protein response (UPR).[7] The UPR is controlled by GRP78 and three major sensors (PERK, IRE1, and ATF6). Studies have shown that temozolomide activates the PERK pathway, leading to sustained ERS and thereby promoting chemoresistance in GBM.[8] Hu *et al*.[9] reported that knocking down CREB3 promotes apoptosis in GBM cells by activating the PERK pathway. These studies indicate that UPR signaling does not linearly promote survival or death; its biological outcome depends on the intensity and duration of stress.[10,11] Additionally, as a critical downstream adaptive mechanism of ERS, autophagy is believed to help clear misfolded proteins and damaged organelles under stress conditions such as hypoxia, thereby alleviating endoplasmic reticulum load and maintaining cellular homeostasis.[12] Research by Bhavya *et al*.[13] supports this role, finding that ERS-induced autophagy protects cells from chemical hypoxia and oxidative damage. However, recent studies have reported that the initiation of autophagy does not necessarily imply enhanced autophagic flux.[14] Previous studies have reported that under certain conditions, an increase in the number of autophagosomes or LC3-II may reflect only initiation events without accompanying complete autophagosome degradation processes. Therefore, it is necessary to combine indicators such as lysosomal inhibition or p62 degradation to assess true flux changes.[15] Singh *et al*.[16] demonstrated that autophagic flux, rather than mere autophagy initiation, is the key determinant of cell fate. However, the mechanisms regulating autophagic flux under ERS conditions in the hypoxic microenvironment of GBM remain unclear.

Inositol-requiring enzyme 1-spliced X-box binding protein 1 (IRE1-XBP1s) is a key branch of the UPR and plays significant roles in endoplasmic reticulum protein homeostasis, membrane biosynthesis, angiogenesis, invasion, and other processes.[17] Studies indicate that the poor prognosis of GBM is associated with tumor cells utilizing the UPR to adapt to stress.[7] For instance, Obacz *et al*.[18] reported that IRE1 promotes UBE2D3 expression through XBP1s, thereby driving myeloid immune cell infiltration in GBM and leading to poor prognosis. Additionally, the IRE1–XBP1s axis can increase the expression levels of autophagy-related genes, thereby coordinating adaptive responses between ERS and autophagy. For example, XBP1s can regulate autophagy levels via a Bcl-2/Beclin-1-associated mechanism.[19] However, a review revealed that under acute or deep hypoxic conditions, IRE1 activity may be inhibited, resulting in decreased or non-significantly increased XBP1s levels.[20] Serine/arginine-rich splicing factor 3 (SRSF3) is a crucial multifunctional splicing factor. High expression of SRSF3 is linked to GBM progression and poor patient prognosis.[21] Notably, SRSF3 deficiency leads to impaired XBP1 splicing, accompanied by reduced levels of active spliced XBP1s.[22] However, in GBM, whether SRSF3 can enhance tumor cell adaptation to hypoxic microenvironments by regulating XBP1 splicing remains unclear. This study aims to investigate this process through related experimental studies.

Materials and Methods

Cell processing

The human astrocyte cell line HA (SNP-H239) and the GBM cell Lines U87 (SNL-096), U251 (SNL-095), A172 (SNL-091), and T98G (SNL-457) were purchased from Shangen Biotechnology (Wuhan, China). They were cultured at 37°C and 5% CO_2 in DMEM-H (C2701; Beyotime, Shanghai, China) supplemented with 10% FBS (C0226; Beyotime) and 1% penicillin/streptomycin (C0222; Beyotime). To investigate the effect of SRSF3 on cell growth, T98G cells were transfected with siRNA targeting SRSF3 (si-SRSF3) or si-NC (GenePharma, Suzhou, China) using Lipofectamine™ 3000 (L3000150; Invitrogen, Carlsbad, CA, USA), and U87 cells were transfected with the pcDNA3.1-SRSF3 overexpression plasmid (OE-SRSF3) constructed by GenePharma, with an empty vector used as a control. After 48 h of incubation, the relevant indicators were measured. To mimic the hypoxic microenvironment of GBM, the cells were allowed to adhere to a normoxic incubator, the medium was replaced with fresh complete medium, and the cells were transferred to a three-gas incubator with premixed gases (1% O_2) for 24 h. Normoxic conditions (21% O_2) were maintained in a standard humidified incubator. To explore the impact of SRSF3 on cells under hypoxia, cells were first transfected with OE-SRSF3 plasmids, and after overexpression was confirmed, hypoxia induction was performed. Finally, to determine whether the role of SRSF3 depends on the IRE1-XBP1s axis, 5 μM[23] of the IRE1 RNase activity inhibitor 4μ8C (412512; Sigma-Aldrich, St. Louis, MO, USA) was added for a 1-h pretreatment following SRSF3 overexpression, followed by 24 h of culture under hypoxic conditions.

CCK-8 assay

A T98G/U87 cell suspension (2×10^3 cells, 100 μL) was inoculated into a 96-well plate. After the cells were precultured in an incubator, 10 μL of CCK-8 solution (CA1210; Solarbio, Beijing, China) was added to each well. The plate was incubated for 4 h, after which the absorbance at 450 nm was measured using a microplate reader.

Colony formation assay

After treatment, the cells were digested with trypsin and evenly seeded into 6-well plates at a density of 200 cells per well. They were placed in a 37°C, 5% CO_2 incubator until visible, appropriately sized colonies formed in the control group (14 days), with 100 μL of medium replenished every 3 days. After the endpoint was reached, the medium was discarded, and the cells were fixed with 4% paraformaldehyde at room temperature for 15 min. Then, 0.1% crystal violet (G1014; Servicebio, Wuhan, China) was added for 5 min of staining. The plates were subsequently washed with running water, and the number of colonies was observed and counted under a microscope.

Transwell assay

Transwell chambers (FTW001; Beyotime) were used for cell

migration and invasion assays. For the cell migration assay, logarithmic-phase cells were collected, washed with serum-free medium, and counted. A 100 µL suspension containing 1×10^4 cells was added to the upper chamber, while 600 µL of medium containing 10% FBS was added to the lower chamber. After 48 hours of incubation, the chambers were removed. The cells on the inner surface of the membrane were wiped off with a cotton swab, fixed with absolute ethanol for 5 min, and then stained with 0.1% crystal violet (G1014; Servicebio, Wuhan, China) for 5 min. After the cells were rinsed with running water and air-dried, images were captured under a microscope, and the cells were counted. The invasion assay differed in that the upper chamber was precoated with diluted Matrigel (356234; Solarbio); the remaining steps were identical to those of the migration assay.

LDH release assay

Cell death was detected using an LDH assay kit (C0016; Beyotime). Briefly, cells were seeded in a 96-well plate at a density of 1×10^4/well and cultured until they reached 80% confluency. After the groups were treated, LDH release reagent was added and incubated for 1 h. The supernatant was then transferred to a new plate by centrifugation at 400 × g for 5 min. Freshly prepared lactate-INT-enzyme mixture working solution was added, and the absorbance at 490 nm was measured after 30 min of incubation at room temperature in the dark. Cell mortality was calculated based on the results.

mRFP-GFP-LC3 staining

Autophagy was detected by observing the formation of autophagosome-fluorescent puncta using an adenovirus labeled with mRFP-GFP-LC3 (GenePharma). Briefly, cells were seeded on confocal dishes and cultured overnight. After transfection with adenovirus (MOI=20, diluted in serum-free medium) for 2 h, the cells were further cultured in complete medium for 48 h. The cells were then gently washed with PBS, fixed with 4% paraformaldehyde, stained with DAPI, and mounted. Analysis was performed using a fluorescence microscope. The fluorescence intensities of the GFP and mRFP channels were analyzed using ImageJ software, and autophagic flux was assessed by the GFP/mRFP ratio.

RT-qPCR

Total RNA was extracted using an RNA isolation kit (AM1912; Invitrogen), and cDNA synthesis and PCR amplification were subsequently performed using a one-step RT–qPCR system (12597500; Thermo Fisher Scientific, Waltham, MA, USA). β-actin was used as the internal reference, and the relative expression levels of genes were calculated using the $2^{-\Delta\Delta CT}$ method. The sequences of the primers used are shown in Table 1.

Semi-quantitative RT-PCR

The changes in XBP1 splicing levels were evaluated through semiquantitative RT-PCR combined with agarose gel electrophoresis. In accordance with the aforementioned experimental methods, total RNA was extracted from U87 cells and then reverse-transcribed to synthesize cDNA. Using cDNA as the template, PCR amplification was performed using a specific primer[24] that spans the IRE1 splicing site. The reaction system used Taq PCR Mix (K1081; Thermo Fisher Scientific), and the number of cycles was controlled during the exponential amplification stage. The PCR products were separated on a 2% agarose gel, and the bands were observed and recorded with a gel imaging system. XBP1u (256) and XBP1s (230) were distinguished based on the size of the PCR products, with β-actin as the internal reference (250). The splicing level of XBP1 was evaluated by comparing the changes in the band intensities of XBP1u and XBP1s in the different treatment groups. The sequences of the primers used are shown in Table 2.

Western blot

The cellular proteins from each group were extracted using RIPA lysis buffer (R0010; Solarbio). The protein concentration was subsequently measured using a BCA kit (23225; Thermo Fisher Scientific). The proteins were separated by SDS-PAGE and transferred to a PVDF membrane (FFP24; Beyotime). The membrane was then blocked with 5% BSA for 1 h, followed by overnight incubation with primary antibodies at 4°C. The primary antibodies used were against the following: SRSF3 (1:1000; ab198291; Abcam, Cambridge, UK), HIF-1α (1:1000; ab179483; Abcam), GRP78 (1:2000; 11587-1-AP; Proteintech, Rosemont, IL, USA), CHOP (1:1000; 15204-1-AP; Proteintech), ATF4 (1:1000; 10835-1-AP; Proteintech), LC3 (1:2000; ab192890; Abcam), p62 (1:1000; ab109012; Abcam), cleaved-caspase3 (1:1000; #9661; Cell Signaling Technology, Inc., Danvers, MA, USA), XBP1u (1:1000; 25997-1-AP; Proteintech), XBP1s (1:1000; 24868-1-AP; Proteintech), and β-actin (1:1000; ab8227; Abcam). After the membrane was washed three times with TBST, it was incubated with an HRP-conjugated secondary antibody (1:2000; ab205718; Abcam) at room temperature for 1 hour. Finally, development was performed using a kit (P0018S; Beyotime). The protein bands were quantified using ImageJ software.

Statistical analysis

GraphPad Prism 8.0 software (La Jolla, CA, USA) was used for data analysis, with measurement data expressed as the mean ±SD. The normality of the data distribution was evaluated through the Shapiro–Wilk test, and the homogeneity of variance was detected using the Levene test. All the data met the statistical assumptions for a normal distribution and homogeneity of vari-

Table 1. Sequences of primers (RT-PCR).

Genes	Forward primer (5'-3')	Reverse primer (5'-3')
SRSF3	GTGTGGGTTGCTAGAAACC	CATAGTGTTCTTCCATCTAGCTC
β-actin	CATGTACGTTGCTATCCAGGC	CTCCTTAATGTCACGCACGAT

Table 2. Sequences of primers (semi-quantitative RT-PCR).

Genes	Forward primer (5'-3')	Reverse primer (5'-3')
XBP1u/s	GGTCTGCTGAGTCCGCAGCA	AAGGGAGGCTGGTAAGGAAC
β-actin	CATGTACGTTGCTATCCAGGC	CTCCTTAATGTCACGCACGAT

ance. Comparisons between two groups were performed using independent samples *t*-tests, and comparisons among multiple groups were conducted using one-way ANOVA with the Tukey test to assess differences between groups. A p-value <0.05 was considered to indicate statistical significance.

Results

SRSF3 is highly expressed in glioma cells

Previous studies have shown that SRSF3 can promote malignant behaviors such as proliferation and invasion in GBM.[21] This study first investigated the expression characteristics of SRSF3 in GBM. Analysis of the TCGA database revealed that the expression of SRSF3 in GBM tissues was significantly greater than that in normal brain tissues (Figure 1A). Furthermore, we examined the expression of SRSF3 in HA cells and the glioma cell lines U87, U251, A172, and T98G. RT-qPCR and Western blot results demonstrated that compared with those in HA cells, the mRNA and protein expression levels of SRSF3 were significantly elevated in all glioma cell lines. Among these cells, T98G cells presented the highest relative expression of SRSF3, whereas U87 cells presented the lowest (Figure 1 B,C). These findings suggest that SRSF3 may play a critical role in the progression of GBM.

SRSF3 promotes the malignant growth of glioma cells

To further investigate the role of SRSF3 in GBM progression, we selected T98G cells, which exhibit the highest SRSF3 expression among glioma cell lines, for SRSF3 knockdown. RT-qPCR and Western blot results demonstrated that SRSF3 knockdown significantly reduced the mRNA and protein expression levels of SRSF3, with si-SRSF3#2 having more pronounced effects (Figure 2 A,B). CCK-8 assays revealed that compared with the si-NC group, the group in which SRSF3 was knocked down had significantly decreased cell viability (Figure 2C). Compared with those in the si-NC group, the number of cell colonies in the SRSF3 knockdown group were markedly decreased, particularly in the si-SRSF3#2 group (Figure 2D). Additionally, SRSF3 knockdown inhibited cell migration and invasion (Figure 2 E,F). We subsequently selected U87 cells, whose glioma cell lines exhibit the lowest SRSF3 expression, for which SRSF3 was overexpressed. RT-qPCR and Western blotting confirmed the transfection efficiency of OE-SRSF3 (Figure 2 G,H). CCK-8 assays revealed that compared with the OE-NC group, the SRSF3-overexpressing group had significantly increased cell viability (Figure 2I). Compared with those in the OE-NC group, the number of colonies in the SRSF3-overexpressing group were significantly increased (Figure 2J). Furthermore, compared with those in the OE-NC group, the migration and invasion abilities of the cells in the SRSF3-overexpressing group were increased (Figure 2 K,L). These results indicate that SRSF3 promotes malignant growth in glioma cells.

Hypoxic glioma cells exhibit increased cell death, accompanied by elevated endoplasmic reticulum stress levels and impaired autophagic flux

Previous studies have shown that hypoxia is a core feature of the GBM microenvironment and can induce ERS and autophagy.[25,26] Therefore, we subjected U87 cells to hypoxic con-

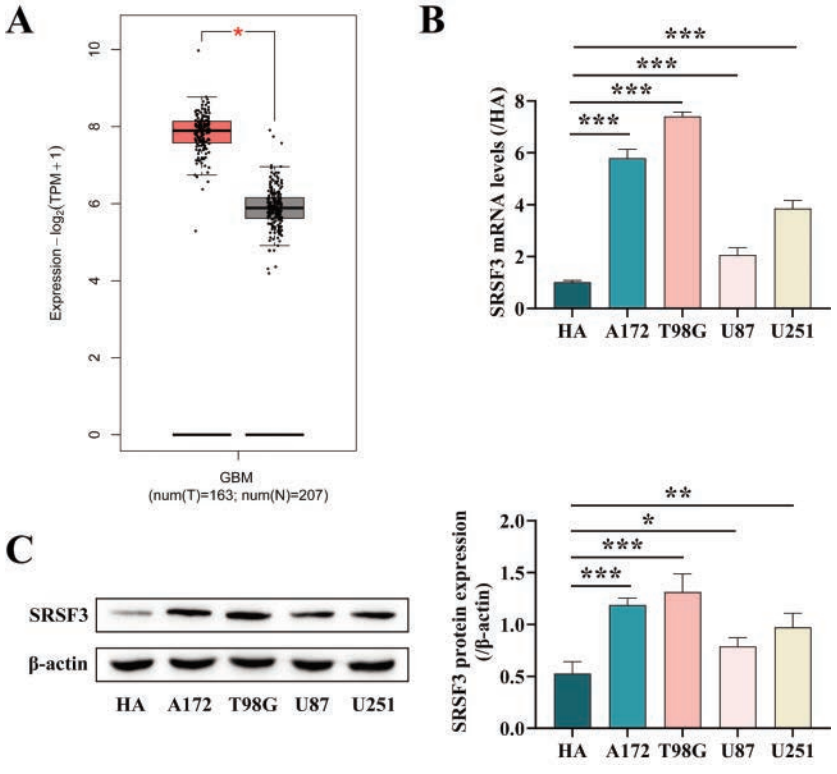

Figure 1. High expression of SRSF3 in glioma cells. **A**) Bioinformatics analysis revealed high expression of SRSF3 in GBM. **B**) RT-qPCR was used to measure the expression of SRSF3 mRNA in each group of cells. **C**) Western blotting was used to measure the expression of SRSF3 in each group of cells. n=3 independent experiments; *p<0.05, **p<0.01, ***p<0.001.

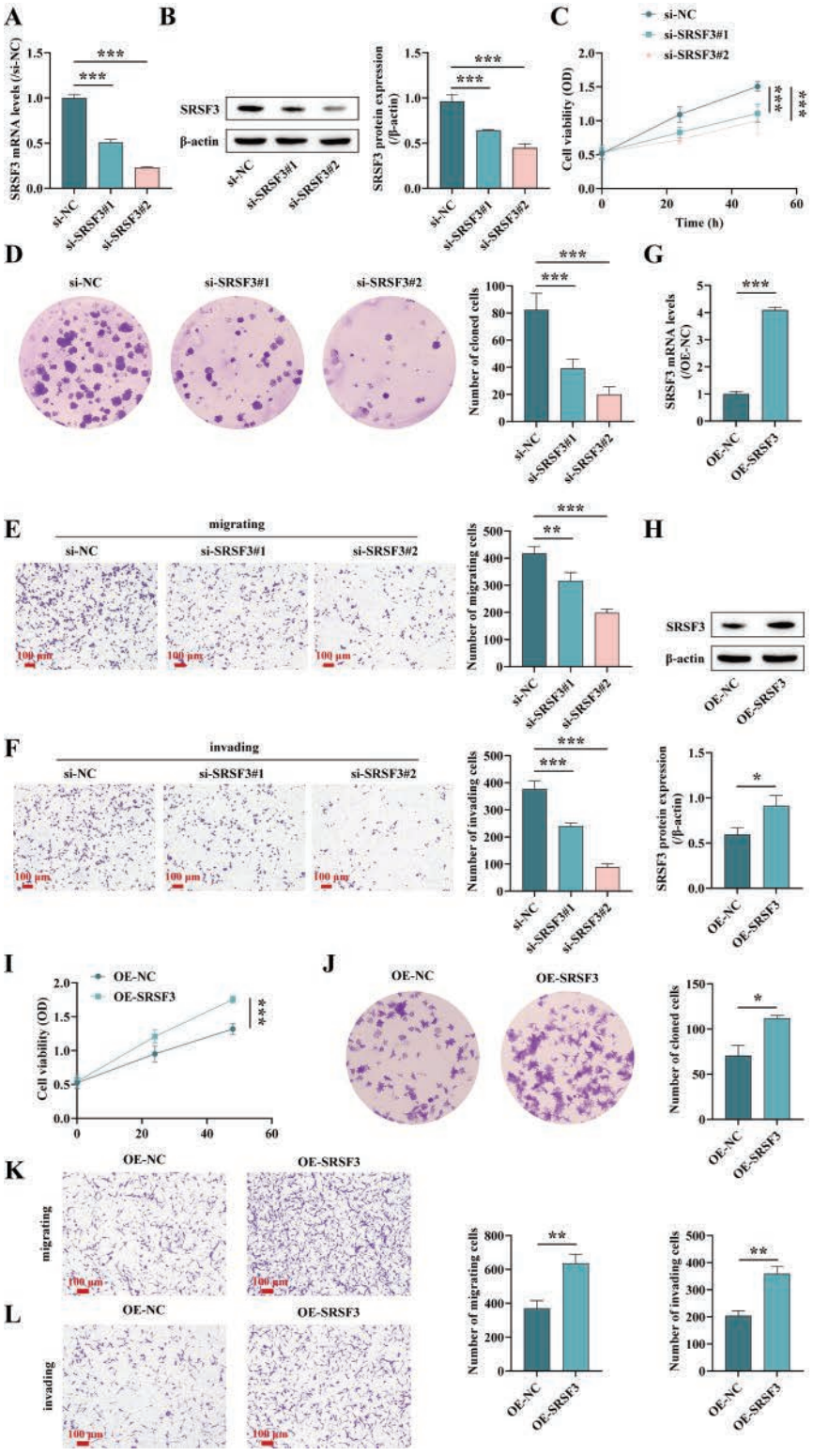

Figure 2. SRSF3 promotes the malignant growth of glioma cells. **A**) RT-qPCR detection of SRSF3 mRNA expression in T98G cells. **B**) Western blot detection of SRSF3 expression in T98G cells. **C**) CCK-8 assay for T98G cell viability. **D**) Colony formation assay to assess the effect of SRSF3 knockdown on T98G cell proliferation. **E**) Transwell assay to evaluate the effect of SRSF3 knockdown on T98G cell migration. **F**) Transwell assay to examine the effect of SRSF3 knockdown on T98G cell invasion. **G**) RT-qPCR detection of SRSF3 mRNA expression in U87 cells. **H**) Western blot detection of SRSF3 protein expression in U87 cells. **I**) CCK-8 assay for U87 cell viability. **J**) Colony formation assay to assess the effect of SRSF3 overexpression on U87 cell proliferation. **K**) Transwell assay to evaluate the effect of SRSF3 overexpression on U87 cell migration. **L**) Transwell assay to examine the effect of SRSF3 overexpression on U87 cell invasion. n=3 independent experiments; *p<0.05, **p<0.01, ***p<0.001.

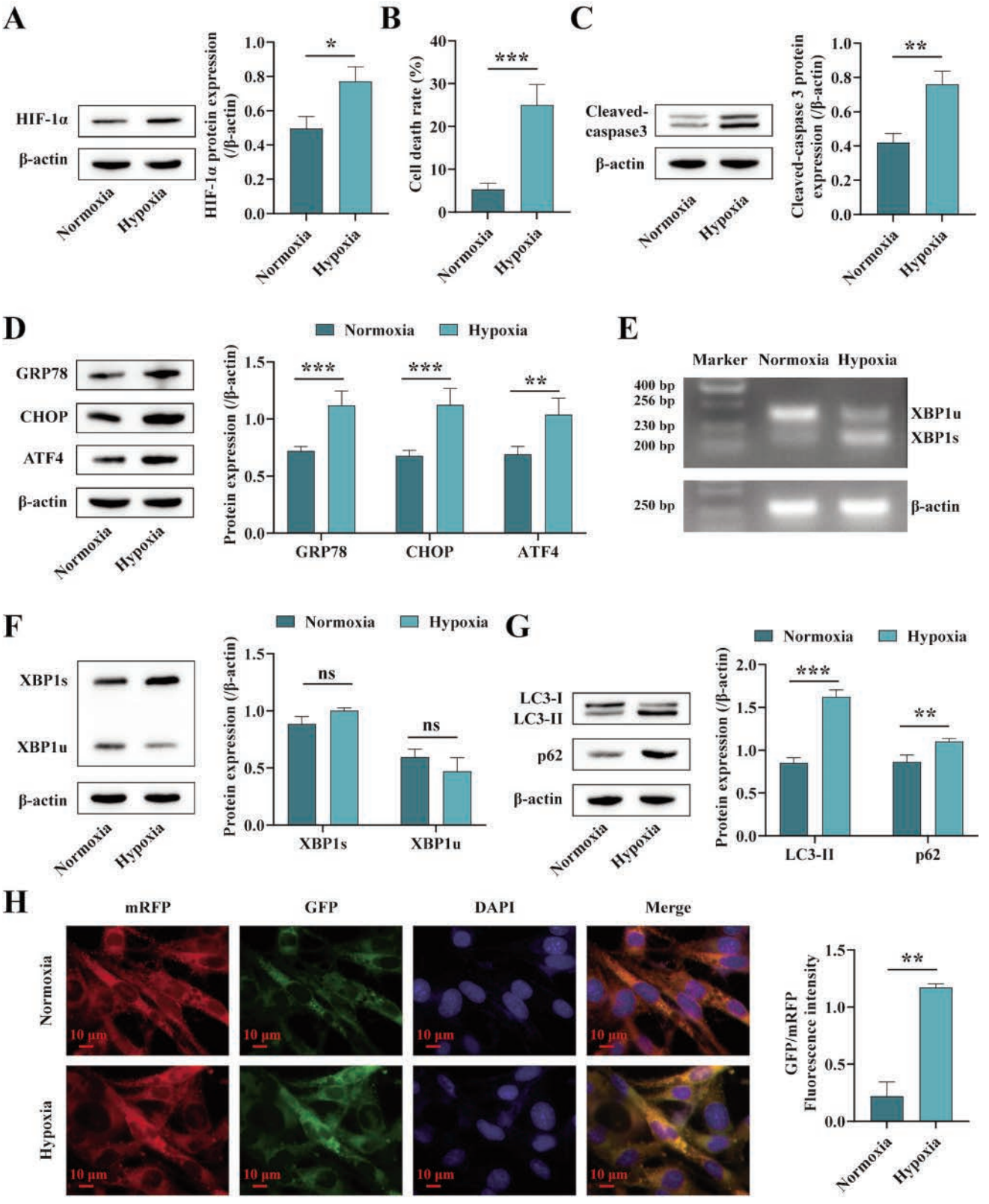

Figure 3. Hypoxic glioma cells exhibit increased cell death accompanied by elevated endoplasmic reticulum stress levels and blocked autophagic flux. **A**) Western blot analysis of HIF-1α expression in U87 cells. **B**) LDH release assay to detect cell death. **C**) Western blot analysis of cleaved-caspase3 expression in U87 cells. **D**) Western blot analysis of GRP78, CHOP, and ATF4 expression in U87 cells. **E**) RT-PCR detection of XBP1u and XBP1s expression. **F**) Western blot analysis of XBP1u and XBP1s expression in U87 cells. **G**) Western blot analysis of LC3-II and p62 expression in U87 cells. **H**) mRFP-GFP-LC3 staining to assess autophagic flux. n=3 independent experiments; *p<0.05, **p<0.01, ***p<0.001.

ditions and detected related indicators. Compared with that in the normoxia group, the expression level of HIF-1α in the hypoxia group was significantly greater (Figure 3A), indicating successful activation of the hypoxia signaling pathway. LDH release assays revealed that 24 hours of hypoxia induction significantly increased the mortality rate of U87 cells (Figure 3B). Additionally, compared with the normoxia group, the hypoxia group presented significantly increased cleaved caspase3 expression (Figure 3C), indicating increased apoptosis. Furthermore, compared with the normoxia group, the hypoxia group exhibited significantly elevated expression levels of GRP78, CHOP, and ATF4 (Figure 3D), suggesting that ERS activation had occurred. RT-PCR and Western blot analyses of XBP1s expression revealed that after 24 h of hypoxia, the expression of XBP1u tended to decrease, whereas the expression of XBP1s tended to increase, but the differences were not significant compared with the expression levels in the normoxia group (Figure 3 E,F). Further detection revealed that hypoxia induction also significantly increased LC3-II and p62 expression (Figure 3G). mRFP-GFP-LC3 staining revealed an elevated GFP/mRFP ratio in U87 cells after 24 h of hypoxia (Figure 3H), indicating impaired autophagic flux. These results suggest that hypoxia induction promotes apoptosis in glioma cells, which is accompanied by elevated ERS levels and blocked autophagic flux.

SRSF3 improves autophagic flux and reduces cell death under hypoxic conditions

In the above study, we confirmed that hypoxia can trigger ERS and block autophagic flux, increasing cell death. Furthermore, we explored the effects of overexpressing SRSF3 on these processes. Compared with the OE-NC group, the SRSF3 overexpression

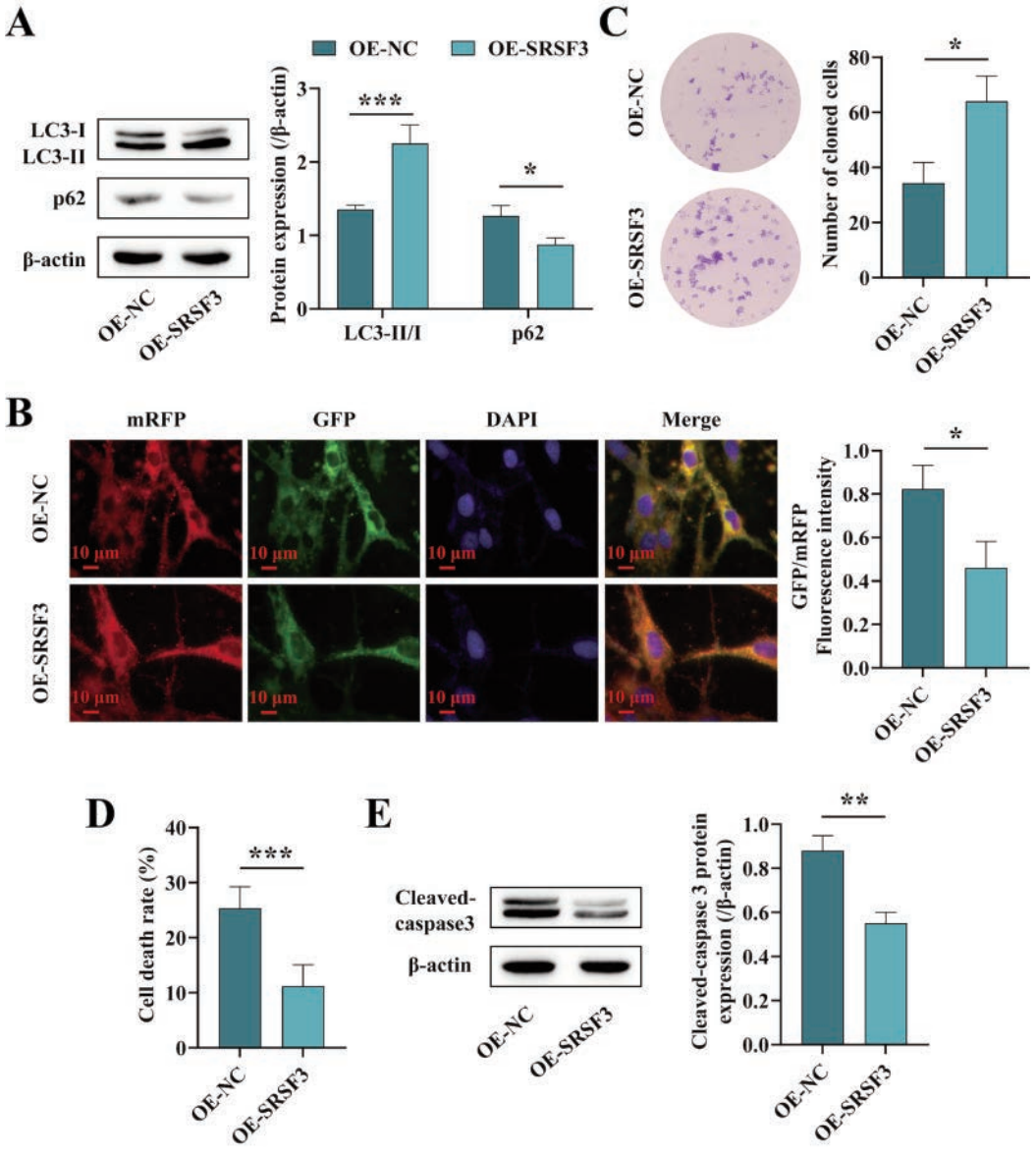

Figure 4. SRSF3 improves autophagic flux and reduces cell death under hypoxic conditions. **A**) Western blotting analysis of the expression levels of LC3-II/I and p62 in U87 cells. **B**) mRFP-GFP-LC3 staining to measure autophagic flux. **C**) Colony formation assay to assess the effect of SRSF3 overexpression on the hypoxia-induced proliferation of U87 cells. **D**) LDH release assay to detect cell death. **E**) Western blotting analysis of cleaved caspase-3 expression in U87 cells. n=3 independent experiments; *p<0.05, **p<0.01, ***p<0.001.

group had a higher LC3-II/I ratio and lower p62 expression (Figure 4A). mRFP-GFP-LC3 staining revealed that SRSF3 overexpression weakened the hypoxia-induced inhibition of autophagic flux and decreased the GFP/mRFP ratio (Figure 4B). Colony formation assays demonstrated that SRSF3 overexpression significantly increased the number of clonogenic cells (Figure 4C). Additionally, the LDH release assay results indicated that SRSF3 overexpression markedly reduced hypoxia-induced cell death in U87 cells (Figure 4D). Western blot results also revealed that compared with the OE-NC group, the SRSF3 overexpression group had significantly decreased cleaved-caspase3 expression (Figure 4E), suggesting reduced apoptosis. These results indicate that SRSF3 can ameliorate hypoxia-induced inhibition of autophagic flux and cell death.

SRSF3 promotes XBP1s formation

Previous studies have shown that XBP1s can promote autophagic flux.[27] As demonstrated above, SRSF3 overexpression restored autophagic flux and reduced cell death. We further investigated whether its molecular mechanism depends on the enhancement of the IRE1-XBP1s axis. Experiments were conducted by adding the IRE1 RNase activity inhibitor 4μ8C to hypoxic U87 cells overexpressing SRSF3. RT–PCR and Western blot results revealed that compared with the OE-NC group, the SRSF3 overexpression group had significantly increased XBP1s expression and decreased XBP1u expression. However, 4μ8C weakened the effects of SRSF3 overexpression on XBP1u and XBP1s expression, increased XBP1u expression and decreased XBP1s expression (Figure 5 A,B). These results indicate that SRSF3 improves autophagic flux and reduces cell death under hypoxic conditions by promoting the formation of XBP1s.

Discussion

GBM is a WHO grade 4 astrocytoma with high incidence and mortality rates and an extremely poor prognosis, posing a significant threat to human life and health.[28] Current GBM treatment still relies primarily on comprehensive therapy, including surgical resection, postoperative radiotherapy, chemotherapy, and other adjuvant treatments. However, owing to issues such as high invasiveness and drug resistance, GBM remains an "almost incurable" malignant tumor.[29] Hypoxia is a core microenvironmental feature of GBM and can drive tumor progression through the remodeling of metabolism, invasion, and stress pathways.[30,31] This study revealed that hypoxia induces ERS in GBM cells and leads to blocked autophagic flux, promoting cell death. SRSF3 is highly expressed in GBM cells and alleviates hypoxia-induced autophagy pathway dysfunction and cell death by promoting the formation of XBP1s. Our research highlights the critical role of SRSF3 in the adaptation of GBM to hypoxia.

Previous studies have suggested that SRSF3 plays a malignant biological role in GBM by promoting proliferation and invasion.[21] In this study, analysis of the TCGA database revealed that the expression of SRSF3 was significantly greater in the GBM group than in the normal group. Similarly, this study revealed that compared with those in HA cells, SRSF3 expression levels in multiple GBM cell lines (U87, U251, A172, and T98G) were markedly greater. These expression profiles suggest that SRSF3 may be functionally related to the development and progression of GBM. SRSF3, the smallest classical splicing factor in the SRSF family, is a multifunctional protein involved in various physiological and pathological processes, including RNA export, RNA translation, and transcriptome integrity.[32] Previous studies have shown that SRSF3 expression is associated with the survival rate of patients with GBM and the expression profiles of related tumor markers and that silencing SRSF3 expression significantly inhibits tumorigenesis and progression.[33] Research by Song *et al*.[21] also demonstrated that SRSF3-regulated alternative RNA splicing promotes GBM tumorigenicity by influencing multiple cellular processes. These studies indicate that SRSF3 acts as an oncogenic factor that drives GBM tumor biology. The results of functional experiments in this study further demonstrated that knocking down SRSF3 under normoxic conditions suppressed T98G cell viability and clonogenic ability and reduced migration and invasion. Conversely, overexpression of SRSF3 enhanced these malignant phenotypes, suggesting that SRSF3 is a regulatory factor that drives glioma cell growth and invasion. Given the ability of SRSF3 to regulate alternative splicing and mRNA metabolism, its pro-malignant effects may be achieved through influencing stress adaptation, metabolic reprogramming, or transcriptional networks related to cell fate.

Hypoxia is among the core features of the GBM microenvironment; hypoxia drives tumor cell invasion, stemness maintenance, and chemotherapy resistance but also poses challenges to cellular protein folding homeostasis.[25,34] For example, in vivo and in vitro studies have shown that hypoxia can upregulate miR-26a through HIF-1α regulation, thereby inhibiting mitochondrial apoptosis and reducing the sensitivity of GBM cells to temozolomide, leading to

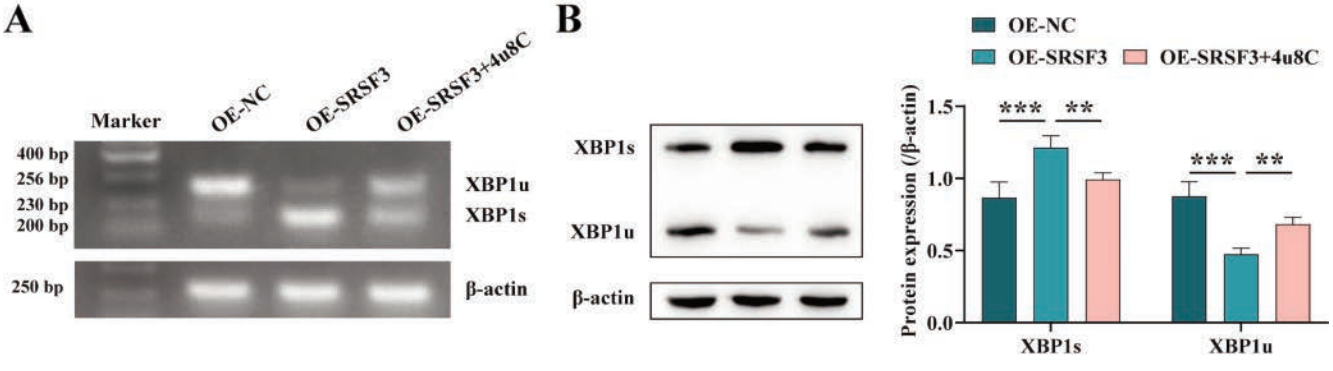

Figure 5. SRSF3 promotes XBP1s formation. **A**) RT–PCR detection of XBP1u and XBP1s expression in each group of cells. **B**) Western blot detection of XBP1u and XBP1s expression in each group of cells. n=3 independent experiments; *p<0.05, **p<0.01, ***p<0.001.

chemotherapy resistance.[35] Other studies have indicated that the UPR is more active in GBM cells than in low-grade gliomas and normal brain tissues, with elevated expression of the three major pathways (PERK, IRE1α, and ATF6) in response to the stress microenvironment.[36] Hypoxia is a key trigger for UPR activation, which promotes short-term cell survival but may also promote apoptosis under sustained severe stress.[37] Our results demonstrated that 24 h of hypoxia significantly increased HIF-1α levels, accompanied by elevated LDH release and cleaved-caspase3 expression, suggesting enhanced apoptosis. Concurrently, the upregulation of ERS markers such as GRP78, CHOP, and ATF4 indicates UPR activation. Additionally, autophagy, as a critical adaptive mechanism to ERS, is tightly coupled with ERS. For instance, in malignant glioma cells, CsA treatment induces ERS while activating autophagy, and inhibition of the ERS pathways PERK and IRE1α partially blocks the autophagic response, highlighting the precursor role of ERS and its clear association with autophagy.[38] Multiple reviews have reported that ERS upregulates autophagy-related gene expression and activity through key UPR branches, whereas autophagy reciprocally modulates ERS intensity, aiding in the clearance of damaged ER fragments to maintain ER homeostasis.[39] This study revealed that autophagy markers exhibit "flux obstruction", as indicated by increased LC3-II/I and p62 expression, along with elevated GFP/mRFP ratios in mRFP-GFP-LC3 fluorescence assays, suggesting impaired autophagosome–lysosome fusion or degradation. This phenomenon indicates that under hypoxic stress, glioma cells exhibit not simply "enhanced autophagy" but rather "increased autophagic initiation/autophagosome formation with impaired terminal degradation," reflecting incomplete autophagy or flux blockade. Thus, the critical determinant of cell fate under hypoxia may not be "whether UPR/autophagy is activated" but rather "whether the adaptive UPR is sufficient and autophagic flux remains intact". Furthermore, by overexpressing SRSF3 in hypoxia-induced U87 cells, we observed that SRSF3 overexpression improved autophagic flux and reduced cell death, demonstrating that SRSF3 promotes GBM cell survival under hypoxia by maintaining autophagic flux.

XBP1s is a noncanonical splicing product mediated by IRE1 and serves as a critical adaptive transcription factor in the UPR; it is capable of inducing molecular chaperones, ER-associated degradation (ERAD), and lipid biosynthesis and enhancing cellular tolerance to protein folding stress.[40] Studies have indicated that XBP1s expression promotes the proliferation and survival of GBM cells. Inhibiting XBP1 splicing not only reduces cell viability but also reverses drug resistance, as demonstrated in temozolomide-resistant GBM cells.[41] Furthermore, XBP1s has been shown to regulate autophagy. For instance, Margariti *et al*.[27] revealed that XBP1s, generated through unconventional splicing of XBP1, directly binds to the BECLIN-1 gene promoter, transcriptionally activates BECLIN-1, and promotes autophagosome formation. However, in the hypoxic tumor microenvironment, the activation and functional efficacy of XBP1s are not always sufficient. A systematic review revealed that acute or severe hypoxia in certain cell types can impair IRE1α activity or hinder the accumulation of XBP1s.[20] Additionally, the output of XBP1s may be regulated by other signaling pathways. Xia *et al*.[42] demonstrated that the Wnt/β-catenin pathway suppresses the functional output of XBP1s under hypoxia. In this study, compared with normoxia, hypoxia induced XBP1 splicing, but the difference was not significant. Given that XBP1s is generated through noncanonical splicing and that the specific loss of SRSF3 leads to a marked reduction in XBP1s protein expression,[22] we propose that the splicing factor SRSF3 may act as a key regulatory node linking hypoxia, ERS, and autophagic flux. Further investigations revealed that SRSF3 overexpression enhances XBP1s production, whereas treatment with 4μ8C attenuates the SRSF3-induced increase in the expression of XBP1s. These results suggest that SRSF3 relies on IRE1 RNase activity to promote the generation of XBP1s from XBP1u, thereby enhancing adaptive UPR output.

This study focuses on stress adaptation mechanisms in the hypoxic microenvironment of GBM and reveals that the splicing factor SRSF3 increases adaptive UPR output by regulating IRE1-dependent XBP1 splicing, thereby maintaining autophagic flux and promoting the survival of GBM cells under hypoxic conditions. However, this study did not clarify whether SRSF3 directly regulates XBP1 pre-mRNA splicing; furthermore, we did not compensate for XBP1s expression in the context of SRSF3 overexpression to verify whether it is sufficient to restore autophagic flux and cell survival, which requires further validation in the future.

References

1. Wu J, Li R, Wang J, Zhu H, Ma Y, You C, et al. Reactive astrocytes in glioma: emerging opportunities and challenges. Int J Mol Sci 2025;26:2907.
2. De Biase G, Garcia DP, Bohnen A, Quiñones-Hinojosa A. Perioperative management of patients with glioblastoma. Neurosurg Clin N Am 2021;32:1-8.
3. Messali A, Villacorta R, Hay JW. A review of the economic burden of glioblastoma and the cost effectiveness of pharmacologic treatments. Pharmacoeconomics 2014;32:1201-12.
4. Chandra A, Young JS, Dalle Ore C, Dayani F, Lau D, Wadhwa H, et al. Insurance type impacts the economic burden and survival of patients with newly diagnosed glioblastoma. J Neurosurg 2019;133:89-99.
5. Domènech M, Hernández A, Plaja A, Martínez-Balibrea E, Balañà C. Hypoxia: the cornerstone of glioblastoma. Int J Mol Sci 2021;22:12608.
6. Pang L, Guo S, Khan F, Dunterman M, Ali H, Liu Y, et al. Hypoxia-driven protease legumain promotes immunosuppression in glioblastoma. Cell Rep Med 2023;4:101238.
7. Yang L, Xue R, Yang C, Lv Y, Li S, Xiang W, et al. Endoplasmic reticulum stress on glioblastoma: Tumor growth promotion and immunosuppression. Int Immunopharmacol 2025;157:114806.
8. Lan B, Zhuang Z, Zhang J, He Y, Wang N, Deng Z, et al. Triggering of endoplasmic reticulum stress via ATF4-SPHK1 signaling promotes glioblastoma invasion and chemoresistance. Cell Death Dis 2024;15:552.
9. Hu Y, Chu L, Liu J, Yu L, Song S, Yang H, et al. Knockdown of CREB3 activates endoplasmic reticulum stress and induces apoptosis in glioblastoma. Aging (Albany, NY) 2019;11:8156-68.
10. Chipurupalli S, Kannan E, Tergaonkar V, D'Andrea R, Robinson N. Hypoxia induced ER stress response as an adaptive mechanism in cancer. Int J Mol Sci 2019;20:749.
11. Hsu S, Chiu C, Dahms H, Chou C, Cheng C, Chang W, et al. Unfolded protein response (UPR) in survival, dormancy, immunosuppression, metastasis, and treatments of cancer cells. Int J Mol Sci 2019;20:2518.
12. Chipurupalli S, Samavedam U, Robinson N. Crosstalk between ER stress, autophagy and inflammation. Front Med (Lausanne) 2021;8:758311.
13. Chandrika BB, Yang C, Ou Y, Feng X, Muhoza D, Holmes AF, et al. Endoplasmic reticulum stress-induced autophagy provides cytoprotection from chemical hypoxia and oxidant injury

and ameliorates renal ischemia-reperfusion injury. Plos One 2015;10:e0140025.
14. Yoshii SR, Mizushima N. Monitoring and measuring autophagy. Int J Mol Sci 2017;18:1865.
15. Follo C, Barbone D, Richards WG, Bueno R, Broaddus VC. Autophagy initiation correlates with the autophagic flux in 3D models of mesothelioma and with patient outcome. Autophagy 2016;12:1180-94.
16. Singh K, Sharma A, Mir MC, Drazba JA, Heston WD, Magi-Galluzzi C, et al. Autophagic flux determines cell death and survival in response to Apo2L/TRAIL (dulanermin). Mol Cancer 2014;13:70.
17. Grandjean JMD, Madhavan A, Cech L, Seguinot BO, Paxman RJ, Smith E, et al. Pharmacologic IRE1/XBP1s activation confers targeted ER proteostasis reprogramming. Nat Chem Biol 2020;16:1052-61.
18. Obacz J, Archambeau J, Lafont E, Nivet M, Martin S, Aubry M, et al. IRE1 endoribonuclease signaling promotes myeloid cell infiltration in glioblastoma. Neuro Oncol 2024;26:858-71.
19. Yan M, Ni J, Song D, Ding M, Huang J. Interplay between unfolded protein response and autophagy promotes tumor drug resistance. Oncol Lett 2015;10:1959-69.
20. Bartoszewska S, Collawn JF, Bartoszewski R. The role of the hypoxia-related unfolded protein response (UPR) in the tumor microenvironment. Cancers 2022;14:4870.
21. Song X, Wan X, Huang T, Zeng C, Sastry N, Wu B, et al. SRSF3-regulated RNA alternative splicing promotes glioblastoma tumorigenicity by affecting multiple cellular processes. Cancer Res 2019;79:5288-301.
22. Sen S, Jumaa H, Webster NJG. Splicing factor SRSF3 is crucial for hepatocyte differentiation and metabolic function. Nat Commun 2013;4:1336.
23. Nelson AM, Carew NT, Smith SM, Milcarek C. RNA splicing in the transition from B cells to antibody-secreting cells: the influences of ELL2, small nuclear RNA, and endoplasmic reticulum stress. J Immunol 2018;201:3073-83.
24. Yoon S, Park Y, Choi S, Yang H, Jeong P, Cha J, et al. Real-time PCR quantification of spliced X-box binding protein 1 (XBP1) using a universal primer method. PLoS One 2019;14:e0219978.
25. García-López D, Zaragoza-Ojeda M, Eguía-Aguilar P, Arenas-Huertero F. Endoplasmic reticulum stress in gliomas: exploiting a dual-effect dysfunction through chemical pharmaceutical compounds and natural derivatives for therapeutical uses. Int J Mol Sci 2024;25:4078.
26. Hu Y, DeLay M, Jahangiri A, Molinaro AM, Rose SD, Carbonell WS, et al. Hypoxia-induced autophagy promotes tumor cell survival and adaptation to antiangiogenic treatment in glioblastoma. Cancer Res 2012;72:1773-83.
27. Margariti A, Li H, Chen T, Martin D, Vizcay-Barrena G, Alam S, et al. XBP1 mRNA splicing triggers an autophagic response in endothelial cells through BECLIN-1 transcriptional activation. J Biol Chem 2013;288:859-72.
28. Schaff LR, Mellinghoff IK. Glioblastoma and other primary brain malignancies in adults: a review. JAMA 2023;329:574-87.
29. Nelson TA, Dietrich J. Investigational treatment strategies in glioblastoma: progress made and barriers to success. Expert Opin Inv Drug 2023;32:921-30.
30. Zhang B, Chen Y, Shi X, Zhou M, Bao L, Hatanpaa KJ, et al. Regulation of branched-chain amino acid metabolism by hypoxia-inducible factor in glioblastoma. Cell Mol Life Sci 2021;78:195-206.
31. Peñaranda Fajardo NM, Meijer C, Kruyt FAE. The endoplasmic reticulum stress/unfolded protein response in gliomagenesis, tumor progression and as a therapeutic target in glioblastoma. Biochem Pharmacol 2016;118:1-8.
32. Zhou Z, Gong Q, Lin Z, Wang Y, Li M, Wang L, et al. Emerging roles of SRSF3 as a therapeutic target for cancer. Front Oncol 2020;10:577636.
33. Fuentes-Fayos AC, Vázquez-Borrego MC, Jiménez-Vacas JM, Bejarano L, Pedraza-Arévalo S, L-López F, et al. Splicing machinery dysregulation drives glioblastoma development/aggressiveness: oncogenic role of SRSF3. Brain 2020;143:3273-93.
34. Li P, Zhou C, Xu L, Xiao H. Hypoxia enhances stemness of cancer stem cells in glioblastoma: an in vitro study. Int J Med Sci 2013;10:399-407.
35. Ge X, Pan M, Wang L, Li W, Jiang C, He J, et al. Hypoxia-mediated mitochondria apoptosis inhibition induces temozolomide treatment resistance through miR-26a/Bad/Bax axis. Cell Death Dis 2018;9:1128.
36. Simbilyabo LZ, Yang L, Wen J, Liu Z. The unfolded protein response machinery in glioblastoma genesis, chemoresistance and as a druggable target. Cns Neurosci Ther 2024;30:e14839.
37. Guan L, Ge R, Ma S. Newsights of endoplasmic reticulum in hypoxia. Biomed Pharmacother 2024;175:116812.
38. Ciechomska IA, Gabrusiewicz K, Szczepankiewicz AA, Kaminska B. Endoplasmic reticulum stress triggers autophagy in malignant glioma cells undergoing cyclosporine a-induced cell death. Oncogene 2013;32:1518-29.
39. Senft D, Ronai ZA. UPR, autophagy, and mitochondria crosstalk underlies the ER stress response. Trends Biochem Sci 2015;40:141-8.
40. Park S, Kang T, So J. Roles of XBP1s in transcriptional regulation of target genes. Biomedicines 2021;9:791.
41. Dowdell A, Marsland M, Faulkner S, Gedye C, Lynam J, Griffin CP, et al. Targeting XBP1 mRNA splicing sensitizes glioblastoma to chemotherapy. FASEB Bioadv 2023;5:211-20.
42. Xia Z, Wu S, Wei X, Liao Y, Yi P, Liu Y, et al. Hypoxic ER stress suppresses β-catenin expression and promotes cooperation between the transcription factors XBP1 and HIF1α for cell survival. J Biol Chem 2019;294:13811-21.

Received: 12 January 2026; Accepted:12 February 2026.

European Journal of Histochemistry 2026; 70:4530
doi:10.4081/ejh.2026.4530